



ELSEVIER

Chemico-Biological Interactions 119–120 (1999) 43–52

Chemico-Biological
Interactions

A preliminary comparison of structural models for catalytic intermediates of acetylcholinesterase

Israel Silman ^{a,*}, Charles B. Millard ^{a,b}, Arie Ordentlich ^c,
Harry M. Greenblatt ^d, Michal Harel ^d, Dov Barak ^c,
Avigdor Shafferman ^c, Joel L. Sussman ^{d,e}

^a Department of Neurobiology, Weizmann Institute of Science, Rehovot 76100, Israel

^b US Army Medical Research Institute of Chemical Defense, Aberdeen Proving Ground,
MD 21010, USA

^c Israel Institute for Biological Research, Ness Ziona 70450, Israel

^d Department of Structural Biology, Weizmann Institute of Science, Rehovot 76100, Israel

^e Biology Department, Brookhaven National Laboratory, Upton, NY 11973, USA

Abstract

Determination of the three dimensional structure of *Torpedo Californica* acetylcholinesterase (*TcAChE*) provided an experimental tool for directly visualizing interaction of AChE with cholinesterase inhibitors of fundamental, pharmacological and toxicological interest. The structure revealed that the active site is located near the bottom of a deep and narrow gorge lined with 14 conserved aromatic amino acids. The structure of a complex of *TcAChE* with the powerful 'transition state analog' inhibitor, TMTFA, suggested that its orientation in the experimentally determined structure was very similar to that proposed for the natural substrate, acetylcholine, by manual docking. The array of enzyme-ligand interactions visualized in the TMTFA complex also are expected to envelope the unstable TI that forms with acetylcholine during acylation, and to sequester it from solvent. In our most recent studies, the crystal structures of several 'aged' conjugates

Abbreviations: ACh, acetylcholine; AChE, acetylcholinesterase (EC 3.1.1.7); BChE, butyrylcholinesterase (EC 3.1.1.8); DFP, diisopropylphosphorofluoridate; MeP-AChE, methylphosphonylated AChE; MES, (2-[*N*-morpholino]ethanesulfonic acid); MiPrP-, monoisopropylphosphoryl; OP, organophosphorus; PEG, polyethylene glycol; *Tc*, *Torpedo californica*; TI, tetrahedral intermediate; TMTFA, *m*-(*N,N,N*-trimethylammonio)-2,2,2-trifluoroacetophenone.

* Corresponding author. Tel.: +972-8-934-2128/3649; fax: +972-8-947-1849.

E-mail address: bnsilm@weizmann.weizmann.ac.il (I. Silman)

0009-2797/99/\$ - see front matter © 1999 Elsevier Science Ireland Ltd. All rights reserved.

PII: S0009-2797(99)00012-5

of *TcAChE* obtained with OP nerve agents have been solved and compared with that of the native enzyme. The methylphosphonylated-enzyme obtained by reaction with soman provides a useful structural analog for the TI that forms during deacylation after the reaction of *TcAChE* with acetylcholine. By comparing these structures, we conclude that the same ‘oxyanion hole’ residues, as well as the aromatic side chains constituting the ‘acyl pocket’, participate in acylation (TMTFA–AChE) and deacylation (OP–AChE), and that AChE can accommodate both TIs at the bottom of the gorge without major conformational movements. © 1999 Elsevier Science Ireland Ltd. All rights reserved.

Keywords: Soman; Trifluoroketones; Tetrahedral intermediate; X-ray crystallography

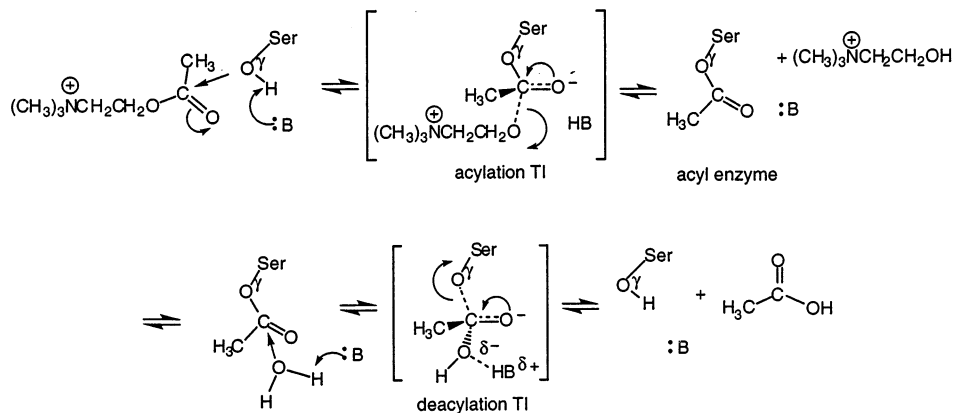
1. Introduction

The three-dimensional structure of acetylcholinesterase (EC 3.1.1.7) from *Torpedo californica* (*TcAChE*) [1], together with kinetic, spectroscopic and site-directed mutagenesis studies, has permitted tentative identification of the amino acid residues that interact with the natural substrate, ACh, during catalysis (reviewed in [2]). The AChE active site presently is believed to possess an oxyanion hole, an acyl binding pocket, and a choline binding site (formerly called the ‘anionic site’). Direct demonstration of these subsites with natural substrates has not yet been achieved because of the inherent instability of the Michaelis complex and the acyl-enzyme. To circumvent this limitation, we are studying the three-dimensional structures of stable enzyme-inhibitor complexes as structural models for intermediates in carboxyl ester hydrolysis.

The reaction of ACh and other carboxyl esters with AChE is believed to proceed through an unstable TI, or through a transition state resembling such a structure, before collapsing to a short-lived ($t_{1/2} \sim 50 \mu\text{s}$) acyl-enzyme [3] (Scheme 1). In the reverse reaction, the acyl-enzyme undergoes nucleophilic attack and proceeds through a second TI or transition state structure, and the regenerated enzyme is expelled as the leaving group (Scheme 1, lower panel).

The trifluoroketone compound, TMTFA (Fig. 1), is a potent inhibitor of AChE (apparent $K_i = 15 \text{ fM}$) which forms a covalent complex with the enzyme, that structurally mimics the theoretical acylation TI [4–6]. The TMTFA–AChE complex, with a trimethylammonium group in the choline binding subsite of the enzyme, is a good analog for the acylation TI of ACh (Scheme 1, upper panel). However, this structure does not address alterations that may occur in the acyl-enzyme, or in the formation of the deacylation TI.

O-pinacolylmethylphosphonofluoridate (soman; Fig. 1) is an OP nerve agent that reacts as a facile ‘hemisubstrate’ of AChE, mobilizing as much as 70% of the enzyme’s natural catalytic power during inhibition [7]. OPs react with AChE to produce a covalent intermediate but, unlike the fleeting acyl-enzyme formed during carboxyl ester hydrolysis, the phosphoenzyme persists for many hours or days (reviewed in [8]). After phosphorylation, soman undergoes a rapid dealkylation reaction, called ‘aging’, to form a monoester anion adduct with the enzyme that is



Scheme 1. Reaction of AChE with ACh. The scheme begins with the reversible enzyme–substrate complex and ends with free enzyme. The top panel shows acylation and the lower panel shows deacylation. The enzyme’s catalytic general base, probably N ϵ 2 of His440, is depicted as :B, and the first product is choline. Hypothetical tetrahedral intermediates are indicated by brackets. Note that the TMTFA complex is expected to resemble the acylation TI (top panel), and the aged OP–AChE conjugate is expected to resemble the deacylation TI (bottom panel).

indefinitely stable [9]. The aged methyl phosphonylated (MeP)-*Tc*AChE complex formed after reaction with soman is expected to share multiple structural features with the unstable ACh deacylation TI [10,11].

In this report, we compare the structure of the TMTFA–*Tc*AChE complex [6] with that of MeP–*Tc*AChE, obtained by reaction with soman [12], with the goal of identifying common topographical features of the theoretical acylation and deacylation TIs formed between ACh and AChE.

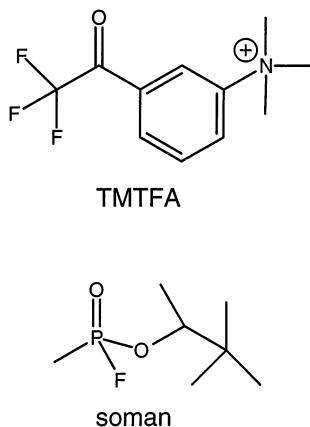


Fig. 1. Chemical structures of soman and TMTFA.

2. Materials and methods

2.1. Determination of MeP-AChE structure

*Tc*AChE was purified from electric organ, essentially as described [13], and the pure enzyme was inhibited with a 2100-fold molar excess of soman. The OP–AChE conjugate was allowed to undergo complete aging in solution. Aging was judged to be greater than 95% complete because no reactivation was observed after incubation in 10 mM pyridine-2-aldoxime methiodide (2-PAM) or 1,1'-trimethylene-bis(4-formylpyridinium bromide) dioxime (TMB-4) for 20 h. Unbound OP was separated from the enzyme by gel filtration, and aged OP–AChE was crystallized using the hanging drop method, with PEG-200 as precipitant in 0.15 M MES buffer, pH 5.8–6.0, 4°C.

The exterior mother liquor which surrounds the crystals during their growth was exchanged with oil to remove water, and the crystals subsequently were flash cooled in liquid nitrogen [14]. Diffraction data were collected at 100 K using a Rigaku Raxis-II camera on a Rigaku rotating anode FR300 generator 'in-house' at the Weizmann Institute (Rehovot, Israel). X-ray diffraction data collection parameters were optimized using the computer program STRATEGY [15], and intensity data were processed with DENZO and SCALEPACK [16]. The OP structure was refined using difference Fourier methods.

2.2. Structure comparison

The coordinates of the TMTFA-*Tc*AChE complex (1ACH) were obtained from the Brookhaven Protein Data Bank. Final refined structures were evaluated and compared using the programs PROCHECK [17] and WHAT-IF [18]. Comparisons of the main chain atom positions for each residue with those of native AChE were performed to identify significant movements using the software PROFIT (SciTech Software, University College, London, UK). Hydrogen positions were calculated and figures generated using the program InsightII v.97.0 (Biosym Technologies, San Diego, CA).

3. Results and discussion

Reaction with soman resulted in an MeP-AChE structure that was refined at 2.2 Å resolution (Fig. 2). The highest positive difference density peak, corresponding to the OP, was observed to be within covalent bonding distance of the O γ of Ser200. As expected, the large molar excess of OP resulted in almost exclusive reaction of AChE with the more toxic, P(S) stereoisomers [19]. No significant change was observed in the positions of the active site triad residues of the MeP–AChE structure compared with those of native AChE or of the TMTFA–AChE complex (Table 1).

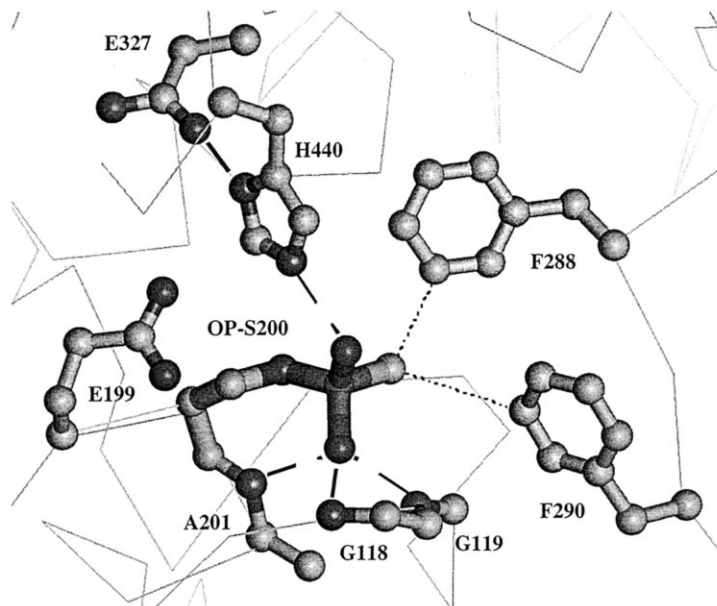


Fig. 2. Three-dimensional structure of the active site of MeP-AChE determined by X-ray crystallography. The conjugate was obtained by reaction of *Tc*AChE with soman. Note the proximity of four possible hydrogen bond donors (dashed lines) to the anionic phosphonyl oxygen atoms: backbone amide nitrogens of A201, G118, and G119, as well as N ϵ 2 of H440. The OP methyl carbon is within non-bonded contact distances (dotted lines) of F288 and F290 in the acyl pocket. For reference, the C α -traces of native- and OP-enzyme are overlaid.

A favorable electrostatic interaction between N ϵ 2 of the active-site imidazolium and one of the oxygen atoms of the anionic OP conjugate was postulated to be a key force in stabilizing aged mono*isopropyl*phosphoryl (*MiPrP*)-trypsin [11,20], as well as *MiPrP*-chymotrypsin [21]. The distance from the N ϵ 2 of His440 to the anionic oxygen in the MeP-AChE structure also is consistent with a favorable interaction [12]. The geometry is consistent with either a coulombic salt bridge or a strong hydrogen bond (Fig. 2).

Table 1
Active site distances in *Tc*AChE structures (Å)

Atom 1	Atom 2	Native AChE	TMTFA complex	MeP-AChE (soman)
S200 O γ	H440 N ϵ 2	2.7	2.7	3.2
H440 N δ 1	E327 O ϵ 1	2.5	2.7	2.4
H440 N δ 1	E327 O ϵ 2	4.4	4.4	4.4
Oxyanion ^a	G119 N	–	2.9	2.4
Oxyanion ^a	G118 N	–	2.9	2.8
Oxyanion ^a	A201 N	–	3.2	3.0

^a Refers to the carbonyl oxygen of TMTFA [6], or the phosphonyl oxygen of soman.

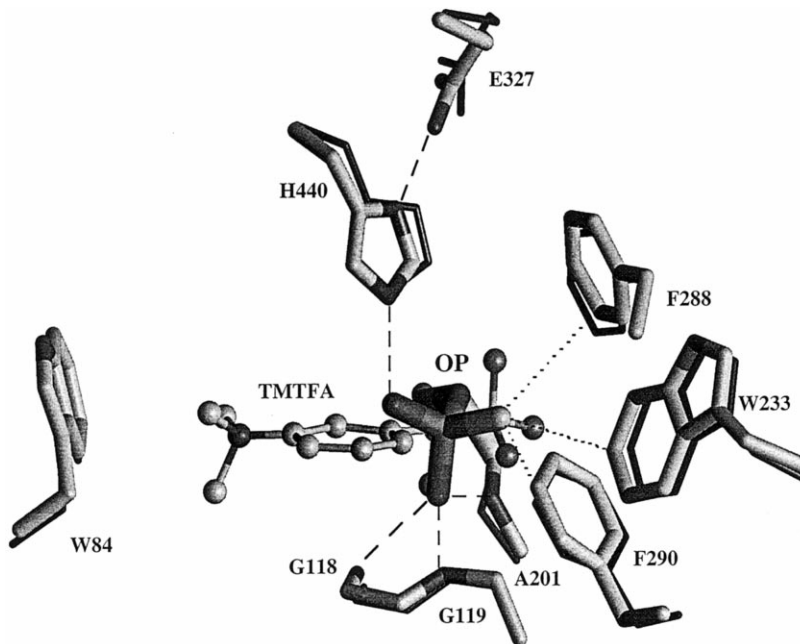


Fig. 3. Comparison of the active sites of MeP-*TcAChE* (soman) and TMTFA-*TcAChE*. The MeP-AChE residues are shown as thick lines, TMTFA-AChE residues are shown as thin dark lines, and TMTFA is shown as a ball-and-stick model. Note that the tetrahedral geometries allow for close superpositioning of the oxyanion hole oxygen atoms (dashed lines indicate potential H-bonds), as well as of the methyl and CF₃ groups in the acyl pocket (dotted lines indicate potential non-bonded contacts).

The phosphonyl oxygen atoms carry significantly greater fractional negative charges than do the oxygens of the ACh deacylation TI [11,22]. Despite this limitation, the active site of MeP-AChE is expected to provide a useful structural analog for modeling steric interactions of the ACh deacylation TI [11,23].

The position of the phosphonyl oxygen should mimic that of the TI carbonyl oxygen. The AChE oxyanion hole has been described as 'three-pronged' [6,24,25] because it has three potential hydrogen bond donors. The MeP-AChE structure corroborates that the oxyanion is stabilized in the deacylation TI by potential hydrogen bonds from the amide nitrogens of G118, G119 and A201 (Fig. 2 and Table 1). This is consistent with preliminary modeling of ACh bound to native *TcAChE* [1], as well as with the structure of TMTFA-*TcAChE* [6]. The carbonyl and phosphonyl oxygen atoms in the oxyanion hole are almost superposable for the TMTFA- and MeP-AChE structures (Fig. 3), as expected from the common tetrahedral geometry in both the acylation and deacylation TI structures. We note that the amide nitrogen atom (donor) of A201 is consistently farther away from the oxygen atom (acceptor) than are those of G118 or G119 (Table 1).

3.1. Acyl pocket

A hydrophobic pocket which surrounds the phosphonate methyl group in the MeP–AChE structure is formed by W233, F288 and F290. The phenyl rings of F288 and F290 provide close non-bonded contacts to the methyl group of soman (Fig. 2 and Table 2). Contacts from the acyl pocket to the phosphonate methyl group are generally closer than are those observed for the CF₃ carbon atom of TMTFA (Table 2). Site-directed mutagenesis studies, along with the TMTFA structure, have emphasized the role of F288 and F290 in determining the specificity of the acyl pocket for different substrates [6,24,26].

Although F288 and F290 have an established role in determining acyl pocket specificity, that of W233 is less clear. Several lines of evidence point to a functional role for W233: (1) both W233 and the adjacent proline (P232) are conserved in all known AChE and BChE sequences; (2) distances from the geometric center of the indole ring to the carbon atom of the CF₃ moiety of TMTFA, as well as to the methyl group of the OP-AChE structure, suggest that W233 is positioned to provide close hydrophobic contacts in the substrate TI (Table 2); and (3) replacement of W233 in human BChE by alanine results in a 30-fold decrease in k_{cat} , with little effect on K_{m} [28]. We also note that the positions of F288 and F290 are flexible and change significantly upon binding of a bulky inhibitor, *diisopropylphosphorofluoridate* (DFP), whereas W233 does not move [12].

It has been proposed that F331 also participates directly in the acyl pocket [6]. The distance of F331 to the methyl group is, however, appreciably greater than are those of F288, F290 or W233 (Table 2). An alternative possibility is that F331 plays a cooperative role in the acyl pocket structure by providing stabilizing π - π -interactions with the key aromatic side chain at F288. This hypothesis could be tested by appropriate double mutant thermodynamic cycles [27,29,30].

Table 2
Acyl pocket distances in *Tc*AChE structures (Å)

From carbon ^a to:	TMTFA complex	MeP-AChE (soman)
F288 ^b	5.1	4.8
F290 ^b	5.6	4.7
W233 ^b	4.8	4.4
F331 ^b	5.6	5.4
G119C α	4.3	3.8

^a Straight line distances from the carbon atom of the phosphonate methyl group, or the carbon atom of the CF₃ group of TMTFA [6].

^b Distances shown are to the geometric center of the phenyl or benzopyrrole rings of the indicated side chain.

3.2. No conformational movement upon binding TI analogs

In the OP–AChE structure, the overall fold of the protein is very similar to that of the native enzyme or the TMTFA–AChE complex, suggesting that *Tc*AChE accommodates the TI for both the acylation and the deacylation reactions at the bottom of the active site gorge without major conformational movements. In contrast, several related serine lipases with extensive secondary structure homology to AChE [31] undergo a major conformational movement of a ‘lid’ region in the protein structure upon reaction with OP transition state analogs [32,33].

Although there is evidence for conformational changes associated with aging of some OP–AChE, –BChE, and -chymotrypsin conjugates in solution [34–36], we found no major structural rearrangements in *Tc*AChE as a result of the aging reaction itself. The rms deviation found by comparing the $C\alpha$ atoms of the MeP-AChE structure with native AChE was less than 0.3 Å. Moreover, superposing the active site residues of MeP-AChE upon those of native *Tc*AChE (Table 1), as well as of 13 other previously solved *Tc*AChE structures, showed no significant movements that could be attributed to aging. It remains possible, however, that a transient conformational change occurred on the pathway to the final aged structure observed by X-ray crystallography. This possibility may be addressed by ongoing X-ray crystallographic studies of OP–AChE complexes that are not aged.

Acknowledgements

This work was supported by the US Army Medical Research & Materiel Command under Agreements No. DAMD17-97-2-7022 and DAMD17-96-C-6088 and the US Army Scientist/Engineer Exchange Program. The opinions or assertions contained herein belong to the authors and are not necessarily the official views of the US Army or the US Department of Defense.

References

- [1] J.L. Sussman, M. Harel, F. Frolow, C. Oefner, A. Goldman, L. Toker, I. Silman, Atomic structure of acetylcholinesterase from *Torpedo californica*: a prototypic acetylcholine-binding protein, *Science* 253 (1991) 872–879.
- [2] P. Taylor, Z. Radic, The cholinesterases: from genes to proteins, *Annu. Rev. Pharmacol. Toxicol.* 34 (1994) 281–320.
- [3] H.C. Froede, I.B. Wilson, Direct determination of acetyl-enzyme intermediate in the acetylcholinesterase-catalyzed hydrolysis of acetylcholine and acetylthiocholine, *J. Biol. Chem.* 259 (1984) 11010–11013.
- [4] U. Brodbeck, K. Schweikert, R. Gentinetta, M. Rottenberg, Fluorinated aldehydes and ketones acting as quasi-substrate inhibitors of acetylcholinesterase, *Biochim. Biophys. Acta* 567 (1979) 357–369.
- [5] H.K. Nair, J. Seravalli, T. Arbuckle, D.M. Quinn, Molecular recognition in acetylcholinesterase catalysis: free-energy correlations for substrate turnover and inhibition by trifluoroketone transition-state analogs, *Biochemistry* 33 (1994) 8566–8576.

- [6] M. Harel, D.M. Quinn, H.K. Nair, I. Silman, J.L. Sussman, The X-ray structure of a transition state analog complex reveals the molecular origins of the catalytic power and substrate specificity of acetylcholinesterase, *J. Am. Chem. Soc.* 118 (1996) 2340–2346.
- [7] I.M. Kovach, J.H.-A. Huber, R.L. Schowen, Catalytic recruitment in the inactivation of acetylcholinesterase by soman: temperature dependence of the solvent isotope effect, *J. Am. Chem. Soc.* 110 (1988) 590–593.
- [8] W.N. Aldridge, E. Reiner, *Enzyme Inhibitors as Substrates: Interactions of Esterases with Esters of Organophosphorus and Carbamic Acids*, vol. 26, North-Holland, Amsterdam, 1972.
- [9] F. Berends, C.H. Posthumus, I.V.D. Sluys, F.A. Deierkauf, The chemical basis of the “ageing process” of DFP-inhibited pseudoacetylcholinesterase, *Biochim. Biophys. Acta* 34 (1959) 576–578.
- [10] Y. Ashani, B.S. Green, Are the organophosphorous inhibitors of acetylcholinesterase transition-state analogs?, in: B.S. Green, Y. Ashani, D. Chipman (Eds.), *Chemical Approaches to Understanding Enzyme Catalysis: Biomimetic Chemistry and Transition*, Elsevier, Amsterdam, 1981, pp. 169–188.
- [11] A.A. Kossiakoff, S.A. Spencer, Direct determination of the protonation states of aspartic acid-102 and histidine-57 in the tetrahedral intermediate of the serine proteases: neutron structure of trypsin, *Biochemistry* 20 (1981) 6462–6474.
- [12] C.B. Millard, G. Kryger, A. Ordentlich, M. Harel, M.L. Ravess, H.M. Greenblatt, Y. Segall, D. Barak, A. Shafferman, I. Silman, J.L. Sussman, Crystal structures of “aged” phosphorylated and phosphonylated *Torpedo californica* acetylcholinesterase, in: B.P. Doctor, D.M. Quinn, R.L. Rotundo, P. Taylor (Eds.), *Structure and Function of Cholinesterases and Related Proteins*, Plenum Press, New York, (1998) pp. 425–431.
- [13] A.H. Futerman, M.G. Low, I. Silman, A hydrophobic dimer of acetylcholinesterase from *Torpedo californica* is solubilized by phosphatidylinositol-specific phospholipase-C, *Neurosci. Lett.* 40 (1983) 85–89.
- [14] H. Hope, Cryocrystallography of biological macromolecules: a generally applicable method, *Acta Crystallogr. (Sect. B)* 44 (1988) 22–26.
- [15] R.B.G. Ravelli, R.M. Sweet, J.M. Skinner, A.J.M. Duisenberg, J. Kroon, STRATEGY: a program to optimize the starting spindle angle and scan range for X-ray data collection, *J. Appl. Cryst.* 30 (1997) 551–554.
- [16] Z. Otwinowski, Oscillation data reduction program, in: L. Sawyer, N. Isaacs, S. Bailey (Eds.), *Data Collection and Processing, Proceedings of the CCP4 Study Weekend of 29–30 January*, SERC, Daresbury, 1993.
- [17] R.A. Laskowski, M.W. MacArthur, D. Moss, J.M. Thornton, PROCHECK: a program to check the stereochemical quality of protein structures, *J. Appl. Cryst.* 26 (1993) 283–291.
- [18] G. Vriend, WHAT IF: a molecular modeling and drug design program, *J. Mol. Graphics* 8 (1990) 52–56.
- [19] H.P. Benschop, L.P.A. deJong, Nerve agent stereoisomers: analysis, isolation, and toxicology, *Acc. Chem. Res.* 21 (1988) 368–374.
- [20] R.M. Stroud, L.M. Kay, R.E. Dickerson, The structure of bovine trypsin: electron density maps of the inhibited enzyme at 5 Å and 2.7 Å resolution, *J. Mol. Biol.* 83 (1974) 185–208.
- [21] M. Harel, C.T. Su, F. Frolow, Y. Ashani, I. Silman, J.L. Sussman, The refined crystal structures of ‘aged’ and ‘non-aged’ organophosphoryl conjugates of γ -chymotrypsin, *J. Mol. Biol.* 221 (1991) 909–918.
- [22] A. Bencsura, I. Enyedy, I.M. Kovach, Origins and diversity of the aging reaction in phosphonate adducts of serine hydrolase enzymes: what characteristics of the active site do they probe?, *Biochemistry* 34 (1995) 8989–8999.
- [23] J. Kraut, Serine proteases: structure and mechanism of catalysis, *Ann. Rev. Biochem.* 46 (1977) 331–358.
- [24] A. Ordentlich, D. Barak, C. Kronman, Y. Flashner, M. Leitner, Y. Segall, N. Ariel, S. Cohen, B. Velan, A. Shafferman, Dissection of the human acetylcholinesterase active center determinants of substrate specificity. Identification of residues constituting the anionic site, the hydrophobic site, and the acyl pocket, *J. Biol. Chem.* 268 (1993) 17083–17095.

- [25] T. Selwood, S.R. Feaster, M.J. States, A.N. Pryor, D.M. Quinn, Parallel mechanisms in acetylcholinesterase-catalyzed hydrolysis of choline esters, *J. Am. Chem. Soc.* 115 (1993) 10477–10482.
- [26] Z. Radic, N.A. Pickering, D.C. Vellom, S. Camp, P. Taylor, Three distinct domains in the cholinesterase molecule confer selectivity for acetyl- and butyrylcholinesterase inhibitors, *Biochemistry* 32 (1993) 12074–12084.
- [27] C.B. Millard, L. Lockridge, C.A. Broomfield, Organophosphorus acid anhydride hydrolase activity in human butyrylcholinesterase: synergy results in a somanase, *Biochemistry* 37 (1998) 237–247.
- [28] P. Masson, P. Legrand, C.F. Bartels, M.-T. Froment, L.M. Schopfer, O. Lockridge, Role of aspartate 70 and tryptophan 82 in binding of succinylthiocholine to human butyrylcholinesterase, *Biochemistry* 36 (1997) 2266–2277.
- [29] G.K. Ackers, F.R. Smith, Effects of site-specific amino acid modification on protein interactions and biological function, *Ann. Rev. Biochem.* 54 (1985) 597–629.
- [30] A. Horovitz, Measures of cooperativity in the binding of ligands to proteins and their relation to non-additivity in protein–protein interactions, *Proc. Royal. Soc. Lond.* B229 (1986) 315–329.
- [31] D.L. Ollis, E. Cheah, M. Cygler, B. Dijkstra, F. Frolow, S.M. Franken, M. Harel, S.J. Remington, I. Silman, J. Schrag, J.L. Sussman, K.V.G. Verschueren, A. Goldman, The α/β hydrolase fold, *Protein Eng.* 5 (1992) 197–211.
- [32] A.M. Brzozowski, U. Derewenda, Z.S. Derewenda, G.G. Dodson, D.M. Lawson, J.P. Turkenburg, F. Bjorkling, B. Hugel-Jensen, S.A. Patkar, L. Thim, A model for interfacial activation in lipases from the structure of a fungal lipase-inhibitor complex, *Nature* 351 (1991) 491–494.
- [33] U. Derewenda, A.M. Brzozowski, D.M. Lawson, Z.S. Derewenda, Catalysis at the interface: the anatomy of a conformational change in a triglyceride lipase, *Biochemistry* 31 (1992) 1532–1541.
- [34] G. Amitai, Y. Ashani, A. Gafni, I. Silman, Novel pyrene containing organophosphates as fluorescent probes for studying aging-induced conformational changes in organophosphate-inhibited acetylcholinesterase, *Biochemistry* 21 (1982) 2060–2069.
- [35] D. Aslanian, P. Grof, F. Renault, P. Masson, Raman spectroscopic study of conjugates of butyrylcholinesterase with organophosphates, *Biochim. Biophys. Acta* 1249 (1995) 37–44.
- [36] N. Steinberg, A.C.M. van der Drift, J. Grunwald, Y. Segall, E. Shirin, E. Haas, Y. Ashani, I. Silman, Conformational differences between aged and non-aged pyrenbutyl-containing organophosphoryl conjugates of chymotrypsin as detected by optical spectroscopy, *Biochemistry* 28 (1989) 1248–1253.